

1 **Design of a Potent D-peptide HIV-1 Entry Inhibitor**
2 **with a Strong Barrier to Resistance***

3
4 Running title: D-peptide HIV Entry Inhibitor

5
6 **Brett D. Welch^{1§}, J. Nicholas Francis^{1§}, Joseph S. Redman¹, Suparna Paul²,**
7 **Matthew T. Weinstock¹, Jacqueline D. Reeves³, Yolanda S. Lie³, Frank G. Whitby¹,**
8 **Debra M. Eckert¹, Christopher P. Hill¹, Michael J. Root², and Michael S. Kay^{1*}**

9 From ¹Department of Biochemistry, University of Utah School of Medicine, Salt Lake
10 City, Utah 84112, ²Department of Biochemistry and Molecular Biology, Thomas
11 Jefferson University, Philadelphia, Pennsylvania 19107, and ³Monogram Biosciences,
12 345 Oyster Point Blvd, South San Francisco, CA 94080.

13
14 [§]These authors contributed equally to this work.

15
16 *Address correspondence to Michael S. Kay, 15 N Medical Drive East Rm 4100, Salt
17 Lake City, UT 84112-5650. Phone: 801-585-5021; Fax: 801-581-7959; E-mail:
18 kay@biochem.utah.edu

19
20 abstract word count: 143

21 text word count: 5803

22
23

1 **Abstract**

2 The HIV gp41 N-trimer “pocket” region is an ideal viral target because it is
3 extracellular, highly conserved, and essential for viral entry. Here, we report the design
4 of a pocket-specific D-peptide, PIE12-trimer, that is extraordinarily elusive to resistance
5 and characterize its inhibitory and structural properties. D-peptides (peptides composed
6 of D-amino acids) are promising therapeutic agents due to their insensitivity to protease
7 degradation. PIE12-trimer was designed using structure-guided mirror-image phage
8 display and linker optimization and is the first D-peptide HIV entry inhibitor with the
9 breadth and potency required for clinical use. PIE12-trimer has ultra-high affinity for the
10 gp41 pocket, providing it with a reserve of binding energy (“resistance capacitor”) that
11 yields a dramatically improved resistance profile compared to other fusion inhibitors.
12 These results demonstrate that the gp41 pocket is an ideal drug target and establish
13 PIE12-trimer as a leading HIV antiviral candidate.

1 **Introduction**

2 The HIV envelope protein (Env) mediates viral entry into cells (11). Env is cleaved
3 into surface (gp120) and transmembrane (gp41) subunits that remain noncovalently
4 associated to form trimeric spikes on the virion surface (16). gp120 recognizes target
5 cells by interacting with cellular receptors, while gp41 mediates membrane fusion.
6 Peptides derived from heptad repeats near the N- and C-terminus of the gp41
7 ectodomain (N- and C-peptides) interact in solution to form a six-helix bundle,
8 representing the post-fusion structure (3, 55, 56). In this structure, N-peptides form a
9 central trimeric coiled coil (N-trimer), creating grooves into which C-peptides bind. This
10 structure, in conjunction with the dominant-negative inhibitory properties of exogenous
11 N- and C-peptides, suggests a mechanism for Env-mediated entry (10, 22, 58-60).

12 During entry, gp41 forms an extended “prehairpin” intermediate that leaves the
13 exposed N-trimer region vulnerable to inhibition for several minutes (18, 35). This
14 intermediate ultimately collapses as the C-peptide regions bind the N-trimer grooves to
15 form a trimer of hairpins (six-helix bundle), juxtaposing viral and cellular membranes
16 and inducing fusion. Fuzeon (enfuvirtide), the only clinically approved HIV fusion
17 inhibitor, is a C-peptide that binds part of the N-trimer groove and prevents six-helix
18 bundle formation in a dominant-negative manner (61). Fuzeon is active in patients with
19 multidrug resistance to other classes of inhibitors and is a life-prolonging option for
20 these patients (30, 31). However, Fuzeon use is restricted to “salvage therapy” due to
21 several limitations including 1) high dosing requirements (90 mg, twice daily injections),
22 2) high cost (~\$30,000/year/patient in the U.S.), and 3) the rapid emergence of resistant
23 strains (21, 47).

1 A deep hydrophobic pocket at the base of the N-trimer groove is an especially
2 attractive inhibitory target because of its high conservation (3, 12, 48), poor tolerance to
3 substitution (4, 34), and critical role in membrane fusion (2). Indeed, this region is
4 conserved at both the amino acid level (for gp41 function in membrane fusion) and the
5 nucleotide level (for the structured RNA region of the Rev-responsive element). Fuzeon
6 binds to the N-trimer groove just N-terminal to the pocket and is significantly more
7 susceptible to resistance mutations than 2nd-generation C-peptide inhibitors, such as T-
8 1249, that also bind the pocket (8, 13, 29, 44, 46, 47, 58).

9 Peptide design, molecular modeling, and small molecule screening have produced a
10 diverse set of compounds that interact with the gp41 pocket and inhibit HIV-1 entry with
11 modest potency, but often with significant cytotoxicity (7, 14, 15, 17, 23, 24, 26, 34, 51,
12 54). The first direct evidence that pocket-specific binders are sufficient to inhibit HIV
13 entry came with the discovery of protease-resistant D-peptides identified using mirror-
14 image phage display (12). In this technique, a phage library is screened against a
15 mirror-image version of the target protein (synthesized using D-amino acids) (50). By
16 symmetry, mirror-images (D-peptides) of the discovered sequences will bind to the
17 natural L-peptide target. As the mirror-images of naturally occurring L-peptides, D-
18 peptides cannot be digested by natural proteases. Protease resistance provides D-
19 peptides theoretical treatment advantages of extended survival in the body and possible
20 oral bioavailability (41, 42, 49).

21 These 1st-generation D-peptide entry inhibitors possess low to mid-micromolar
22 potency against a lab-adapted isolate (HXB2) (12). We previously reported an affinity-
23 matured 2nd-generation D-peptide pocket-specific inhibitor of entry called PIE7 (57). A

1 trimeric version of PIE7 is the first high affinity pocket-specific HIV-1 inhibitor and has
2 sub-nM potency against X4-tropic (HXB2) and R5-tropic (BaL) strains. However,
3 significant further optimization is required to create a robust clinical candidate for two
4 reasons. First, this D-peptide is much less potent (high nM) against JRFL, a primary R5-
5 tropic strain. Therefore, improved PIE potency is necessary to combat diverse primary
6 strains. Second, by improving the affinity of our inhibitors for the pocket target, we hope
7 to provide a reserve of binding energy that will delay the emergence of drug resistance,
8 as described below.

9 We and others have reported a potency plateau for some gp41-based fusion
10 inhibitors that is likely imposed by the transient exposure of the prehairpin intermediate
11 (9, 27, 53, 57). For very high affinity inhibitors, association kinetics (rather than affinity)
12 limits potency so that two inhibitors with significantly different affinities for the prehairpin
13 intermediate can have similar antiviral potency. We proposed that “over-engineering”
14 our D-peptides with substantial affinity beyond this potency plateau would provide a
15 reserve of binding energy that would combat affinity-disrupting resistance mutations
16 (57). Such a “resistance capacitor” should also prevent the step-wise accumulation of
17 subtle resistance mutations in Env by eliminating the selective advantage such mutants
18 would otherwise confer.

19 Here, we report the design and characterization of a 3rd-generation pocket-specific
20 D-peptide, PIE12-trimer, with ~100,000-fold improved target binding compared to the
21 best previous generation D-peptide, significantly broadened inhibitory potency, and an
22 enhanced resistance capacitor that provides a strong barrier to viral resistance. We
23 achieved this increased potency via structure-guided phage display and crosslinker

1 optimization. PIE12-trimer has a dramatically improved resistance profile compared to
2 earlier D-peptides, as well as Fuzeon and T-1249. These results validate the resistance
3 capacitor hypothesis and establish PIE12-trimer as a leading anti-HIV therapeutic
4 candidate.

5

6 **Results**

7 **Structure-guided phage display to optimize flanking residues**

8 PIE inhibitors consist of a short core sequence surrounded by a disulfide bond that
9 imparts structural rigidity required for binding (Table 1) (12). The large jump in affinity
10 between our 1st (12) and 2nd-generation (57) inhibitors was accomplished by optimizing
11 this core sequence. There were also four fixed “flanking” residues outside the disulfide
12 that arose from phage library cloning restrictions, Gly-Ala on the N-terminus and Ala-Ala
13 on the C-terminus. Interestingly, our co-crystal structures of D-peptides in complex with
14 a mimic of its gp41 pocket target (IQN17) reveal significant contacts between these
15 presumed inert flanking residues and the pocket (12, 57). Thus, we reasoned that their
16 optimization would likely lead to improved D-peptide affinity for the pocket.

17 To optimize these flanking residues, we used a commercially available phage library
18 cloning system (NEB) that allowed us to relocate cloning sites away from the flanking
19 regions (38). We redesigned the regions immediately outside the flanking residues in
20 our cloning vector in order to structurally isolate them and minimize any bias caused by
21 flanking sequence randomization. Using this vector, we constructed a phage library that
22 varied only these four residues in the context of our previously optimized PIE7 core
23 sequence (XXCDYPEWQWLCXX). After four rounds of panning, our phage library

1 showed ~100-fold improved binding to a gp41 pocket mimic (IZN17) compared to clonal
2 PIE7-phage with the original GA/AA flanking sequence. We extensively sequenced this
3 phage pool to identify a consensus sequence, H(A/P)-[PIE7 core]-(R/K/E)L, as well as
4 five dominant individual sequences. Using a phage clone binding assay we found that
5 these sequences bound the gp41 pocket 70 – 900-fold more tightly than PIE7, with
6 PIE12 (HP-[PIE7 core]-EL) having the highest affinity (data not shown).

8 **Enhanced potency of 3rd-generation D-peptides**

9 We synthesized D-peptides corresponding to the top three phage sequences in the
10 binding assay (PIE12 – PIE14) and tested their antiviral potency in a pseudovirion entry
11 assay (Table 1 and Fig. 1). Pairwise comparisons of both phage binding and inhibitor
12 potency indicate that Pro is preferred over Ala at position 2 and Glu is preferred over
13 Arg or Lys at position 13. As predicted from the phage binding assay, PIE12 has the
14 best potency and is ~40-fold more potent than PIE7 (our best previously reported
15 monomer) against JRFL.

17 **Crystal structure of PIE12**

18 To better understand the sources of PIE12's improved binding and potency, we
19 crystallized PIE12 in complex with the N-trimer pocket mimic IQN17. Data were
20 collected from three crystal forms (Table 2) at between 1.45 and 1.55 Å resolution. Each
21 IQN17 trimer from the three crystal forms reported here and from the PIE7 structure
22 (pdb code 2R5D) agreed well with one another (rmsd 0.6 to 1.2 Å) based on least
23 squares overlap on all C α atoms (residues 1-45 of all three chains). The structures

1 suggest two sources of the improved affinity of PIE12 for IQN17 compared to PIE7.
2 First, the new N-terminal flank residues (His1 and Pro2) form favorable ring stacking
3 interactions with the pocket (IQN17-Trp571) (Fig. 2). Second, the substitution of Leu for
4 Ala in the C-terminal flank sequence buries an additional $\sim 50 \text{ \AA}^2$ hydrophobic surface
5 area in the pocket. Neither of these new interactions with the flanking sequence
6 perturbs the original pocket binding structure of the core PIE7 residues. Importantly, the
7 structures reveal that PIE12's improved affinity does not result from new interactions
8 with less conserved regions outside of the pocket that might render PIE12 more
9 vulnerable to resistance mutations.

10

11 **Discovery and structure of a 7-mer D-peptide**

12 The core sequence of PIE7 and PIE12 comprises 8 residues flanked by cysteines (8-
13 mer). Modeling based on our 8-mer D-peptide/IQN17 crystal structures suggests that a
14 7-mer core is compatible with pocket binding of the WXWL consensus and formation of
15 a disulfide bond (57). Previously, we saw that decreasing the size of the PIE core (from
16 10 residues to 8) led to dramatically increased pocket binding (57), so we reasoned that
17 further decreasing the size of the core might lead to additional potency gains. To
18 explore this alternative geometry, we used a similar mirror-image discovery process as
19 employed with 8-mers to identify a 7-mer, PIE71 (FVCPPEWRWLCDL). PIE71 contains
20 the same WXWL motif as found in 8-mer and 10-mer pocket binders and inhibits HXB2
21 entry with an IC_{50} value of 410 nM (data not shown), ~ 1.5 fold better than PIE7, but an
22 order of magnitude worse than PIE12.

1 To gain a better understanding of the 7-mer binding solution, we determined a co-
2 crystal structure of PIE71 in complex with IQN17 (Table 2). The key residues involved in
3 the binding interface (WXWL) adopt nearly superposable conformations to those
4 observed in PIE7 and PIE12, as do the C-terminal flank residues. However, the two
5 structures deviate significantly at the N-terminus (Figs. 2 and 3). Specifically, the 7-
6 mer's disulfide bond is shifted much closer to the pocket, which directs the N-terminal
7 flank residues away from the pocket region. As a result, the N-terminal flanking residues
8 (Phe-Val) only graze the pocket, compared to the intimate interaction of PIE12's N-
9 terminal flanking residues. So although the 7-mer is compatible with pocket binding, the
10 smaller core is too constrained to allow optimal binding of the flank residues to the
11 pocket. Due to this decreased binding interface and therefore decreased potency, we
12 decided not to pursue the 7-mer geometry further.

13

14 **Optimization of crosslinker length and geometry**

15 We previously took advantage of the trimeric nature of the gp41 pocket target to
16 geometrically increase PIE7 binding affinity by crosslinking it into dimers and trimers
17 (57). PIE7 has an N-terminal lysine, which furnishes a unique primary amino group (the
18 N-terminus is acetylated) and was added for solubility. This lysine was used to produce
19 dimers via reaction with a bis(NHS ester)PEG crosslinker (NHS esters selectively react
20 with primary amino groups). Trimers were produced by crosslinking two PIE7s to a
21 central peptide with two lysines at the N-terminus (2K-PIE7).

22 We hypothesized that the strength of the avidity effect is related to the length of the
23 crosslinker and that shorter crosslinkers that still allow simultaneous binding to multiple

1 pockets could strengthen potency. For the original N- to N-terminal linkage, we used a
2 crosslinker with a ~35 Å spacer arm consisting of 9 PEG units (N₉N linkage). However,
3 our crystal structures of D-peptides in complex with IQN17 reveal that C- to C-terminal
4 or N- to C-terminal linkages could be significantly shorter and could be spanned by a
5 ~22 Å crosslinker whose spacer arm consists of 5 PEGs (C₅C and N₅C linkages).
6 Therefore, we relocated Lys to the C-terminus of PIE7 (PIE7-GK) in order to make the
7 N₅C hetero- and C₅C homodimers (see Materials and Methods for additional details).

8 The resulting N₅C- and C₅C-PIE7 dimers have similar potencies that are significantly
9 enhanced compared to our previous N₉N-PIE7 dimer (Table 1 and Fig. 4A). Based on
10 these data, we chose C₅C connections as our standard linker, since they are simpler to
11 produce than the hetero N₅C linkage. Hereafter, all dimers and trimers use the C₅C
12 linkage unless otherwise specified. Combining our new optimized flanking residues and
13 linkages, we produced PIE12-dimer and trimer. Both are extremely potent against the
14 difficult-to-inhibit primary strain JRFL (low nM IC₅₀s; Fig. 4B, Table 1), up to two orders
15 of magnitude more potent than our best previously described D-peptide (N₉N PIE7-
16 trimer) (57).

17

18 **Breadth against a diverse multiclade panel**

19 HIV-1 has jumped from chimpanzees to humans at least three separate times giving
20 rise to groups M, N, and O (19). The main group (group M), accounts for >99% of all
21 HIV-1 infections worldwide (32). HIV's high mutation rate has led to the emergence of
22 diverse subtypes within Group M that are categorized as clades A-D, F-H, J, K, and
23 various circulating recombinant forms (CRFs, e.g., AE and BF). In 2000, clades A-D

1 were estimated to represent >90% of HIV infections (39); however, in recent years
2 CRFs have become more prevalent (1). Different subtypes contain up to 35% sequence
3 diversity in Env, often causing antibodies raised against a particular strain to be
4 ineffective against others (20).

5 To ensure that our pocket-specific D-peptides are potent and broadly neutralizing
6 against the most common subtypes of HIV, we measured the potency of PIE7-trimer,
7 PIE12-trimer, and PIE12 (with Fuzeon as a control inhibitor) using the PhenoSense
8 Entry® pseudovirion assay (Monogram Biosciences, Table 3) (43). The inhibitors were
9 tested against a panel of 23 viruses pseudotyped with clonal and polyclonal envelopes
10 representing clades A-D, several CRFs, and Fuzeon-resistant strains. Both PIE7- and
11 PIE12-trimers potently inhibited all strains tested, though PIE12-trimer was generally a
12 superior inhibitor (and in all cases more potent than Fuzeon). While PIE12-monomer is
13 much less potent than the trimer, it is also broadly active. Interestingly, PIE12-trimer is
14 ~10-fold more potent than the PIE7-trimer against polyclonal virus from clades B and C
15 (samples amplified from patient plasma), which is consistent with a resistance capacitor
16 mechanism for maintaining potency in the presence of varying Env sequences. All of
17 the D-peptide inhibitors are unaffected by Fuzeon resistance mutations. Additionally,
18 lack of inhibition against a murine leukemia virus (MLV) control indicates that these
19 inhibitors are specific and nontoxic in this assay.

20

21 **Breadth against replication-competent primary viral isolates on PBMCs**

22 To more closely mimic *in vivo* infection and further establish inhibitory breadth, we
23 also tested the ability of PIE7-trimer, PIE12-trimer, and PIE12 to inhibit PBMC infection

1 by replicating primary strains, again with Fuzeon as a control (Table 4). These data
2 confirm the potent and broad inhibitory activity of PIE7- and PIE12-trimer against all
3 group M strains tested including several CRFs. Toxicity was not observed on these cells
4 at inhibitor concentrations up to 1 μ M (highest concentration tested), demonstrating a
5 high therapeutic index for the trimers. Interestingly, the inhibitors are more potent in this
6 assay than in the PhenoSense Entry assay, which may be due to differential receptor
7 expression levels between the two cell types (45).

8 Notably, two group O strains were also tested in this assay and are much less
9 sensitive to inhibition than group M strains. Group O contains several mutations
10 (compared to group M) in the pocket including: Q567R, T569S, K574R, Q577R, and
11 V580L. The crystal structures of PIE7 and PIE12 in complex with IQN17 reveal that, of
12 these residues, the D-peptide directly interacts only with K574 (via a hydrophobic
13 interaction) and Q577 (via hydrogen bonds). Group O gp41 has several other mutations
14 in the groove just outside the pocket (i.e., H564E) that could also affect PIE potency
15 (e.g., by slowing the association rate). It will be interesting to analyze the effects of
16 these mutations in a group M (e.g., HXB2 or JRFL) background to see if they are
17 responsible for the loss of potency.

18

19 **Evidence for a charged “resistance capacitor”**

20 With the design of PIE12-trimer, we now observe strong evidence for a highly
21 charged resistance capacitor in which the PIE12-trimer pocket-binding affinity vastly
22 exceeds the inhibitory potency. Comparing PIE7- and PIE12-trimers, we observe similar
23 potencies against pseudovirion entry (Fig. 4B, Table 1), although we expect their target
24 affinities to be extremely different.

1 Due to extraordinarily slow off-rates, direct measurements of the pocket affinities for
2 PIE7- and PIE12-trimers via surface plasmon resonance, as used for earlier generation
3 D-peptides (57), were not possible. Since binding affinity of inhibitors correlates to the
4 stability of inhibitor-target complexes, we used thermal denaturation monitored by
5 circular dichroism (CD) to measure the relative stabilities of each IZN17-inhibitor
6 complex and infer the relative affinities of our ultra-high affinity binders. The melts were
7 performed in 2 M GuHCl to destabilize the complexes and shift their melting points into
8 an observable range (below 100 °C).

9 The normalized thermal melts for each IZN17/inhibitor complex are plotted in Fig. 5
10 with T_m values shown in the legend. As expected, PIE12-trimer forms the most stable
11 complex and has a T_m 8 °C higher than the next most stable inhibitor complex (PIE7-
12 trimer). The PIE12 monomer also forms a more stable complex than the PIE7
13 monomer, as expected. Our previous experience showed that improvements in
14 monomer affinity translated to approximately squared and cubed improvements in the
15 corresponding dimers and trimers (57). Based on PIE12-trimer's optimized C₅C linkage
16 (35-fold improved in antiviral potency over N₉N linkage, JRFL data) and the ~25-fold
17 difference in monomer potency between PIE7 and PIE12 (JRFL data), we estimate that
18 PIE12-trimer binds to gp41 >10⁵-fold (35*25³) more tightly than (N₉N)PIE7-trimer. This
19 predicted sub-fM binding translates to a resistance capacitor charged to ~6 kcal/mol
20 against JRFL. Interestingly, the potency plateau lies at a slightly better potency for
21 trimers compared to dimers, likely due to their faster association rates (i.e., three vs. two
22 opportunities for initial collision with target).

23

1 **Selection of Resistant Strains**

2 To measure the resistance profile of our D-peptide inhibitors and test our resistance
3 capacitor hypothesis, we conducted viral passaging studies with escalating inhibitor
4 concentration to select for resistant strains. These studies initially used PIE7-dimer,
5 which was available from our previous study (57) and inhibits the parental strain, NL4-3,
6 with an IC_{50} of ~20 nM. By doubling PIE7-dimer concentration every 2 to 3 weeks, we
7 obtained stable viral cultures in 2000 nM inhibitor within 20 weeks of propagation. In
8 comparison, we were able to obtain high-level Fuzeon-resistance (>1000-fold) in only
9 ~3 weeks using a similar protocol (Steger HK, et al., submitted).

10 Sequencing the N-peptide region of PIE7-dimer resistant viruses revealed two
11 selected mutations: E560K and V570I. These substitutions in context of HXB2
12 pseudovirions conferred ~400-fold resistance to PIE7-dimer. These mutations also
13 dramatically weaken the binding of D-peptides to the gp41 pocket, but not the C-peptide
14 inhibitor C37 (Root et al., unpublished data). It is not obvious from the PIE7 structure
15 how these mutations weaken PIE7 binding. Despite this loss of affinity, the escape
16 mutations had minimal effect on the potencies of PIE12-dimer and PIE12-trimer, as well
17 as the C37 control inhibitor (Fig. 6). This result is predicted by the resistance capacitor
18 hypothesis: affinity-disrupting escape mutations selected in the presence of weaker
19 binding inhibitors should be less disruptive to the potencies of tighter binding inhibitors.

20 The rapid inhibitor escalation strategy utilized to generate PIE7-dimer resistance was
21 not effective in generating HIV-1 resistant to PIE12-dimer or PIE12-trimer. Rather, HIV-
22 1 titer fell precipitously when inhibitor concentrations exceeded 20 nM (5 to 20x IC_{50}).
23 Instead, we switched to a much slower escalation strategy, with prolonged periods at

1 stable inhibitor concentrations (5-15 weeks). Resistant virus emerged after 40 weeks of
2 propagation in PIE12-dimer and after 65 weeks of propagation in PIE12-trimer. These
3 observations suggest that a strong resistance capacitor profoundly delays selection of
4 resistance mutations for these optimized fusion inhibitors.

5 Sequencing of the pocket region of PIE12-trimer resistant viruses reveals only one
6 mutation, Q577R. Interestingly, this substitution is present in nearly all group O isolates
7 (including BCF01 and BCF02, Table 4), but rare among group M isolates.
8 Pseudovirions bearing Q577R confirm that this mutation confers substantial resistance
9 to PIE12-trimer (data not shown). Examination of the PIE12 crystal structure shows that
10 Q577 makes hydrogen bonds with Glu7 and Trp10 in PIE12, which may explain the
11 disruptive effects of this mutation. Q577R's codon is predicted to disrupt the RRE stem-
12 loop V structure since it base pairs with the invariant W571 codon (Trp is only encoded
13 by one codon).

1 **Discussion**

2 PIE12-trimer is a D-peptide entry inhibitor with ~80-fold enhanced potency and an
3 estimated >100,000-fold improved binding affinity compared to the best previously
4 reported D-peptide. This dramatic improvement in affinity produces excellent breadth
5 and a charged resistance capacitor to combat the emergence of resistance mutations.
6 Indeed, PIE12-trimer was able to withstand the impact of resistance mutations to earlier
7 generation D-peptides and required a much longer selection (65 weeks) to generate
8 resistant stains. Ongoing work is exploring the mechanism of PIE7-dimer, PIE12-dimer,
9 and PIE12-trimer resistance and its relationship to group O's insensitivity. A key
10 question is whether HIV can develop resistance against these inhibitors independent of
11 changes in affinity (e.g., kinetics) that are capable of maintaining viral fitness.

12 Viral escape affects even the newest class of FDA-approved HIV-1 drugs, integrase
13 inhibitors. Resistance to raltegravir and corresponding treatment failure was observed in
14 a significant subset of patients in both the Phase II and III clinical studies (5), and
15 corresponding resistance mutations can be seen within 4 weeks when selected in viral
16 passaging studies (28). Our studies indicate that PIE12-trimer is a promising entry
17 inhibitor that could overcome limitations associated with the two currently approved
18 entry inhibitors, Fuzeon (high dosing, susceptibility to resistance) and
19 Selzentry/maraviroc (only effective against R5 viruses), and may also prove to have a
20 better resistance profile than even the newest class of HIV-1 inhibitors.

21 In addition to a possible therapeutic agent, PIE12-trimer is an ideal candidate for a
22 topical microbicide, as its protease resistance would allow it to withstand the protease-
23 rich environment of the vaginal mucosa. In the absence of a safe and effective HIV

1 vaccine, a topical microbicide to prevent the sexual transmission of HIV is an urgent
2 unmet global health need. The ultimate utility of PIE12-trimer as a microbicide or
3 therapeutic agent will be determined by advanced pre-clinical and clinical studies,
4 including characterization of pharmacokinetics, *in vivo* toxicity, effectiveness in animal
5 models of HIV infection (alone or in combination with other HIV inhibitors), and
6 optimization of formulations for microbicide gels or vaginal rings.

7 More generally, this work unequivocally shows that D-peptide inhibitors can be
8 designed with high potency and specificity against natural L-protein targets. The D-
9 peptide design methodology described here can be applied to diverse biomedical
10 applications, particularly for the many viruses that share HIV's hairpin-closing entry
11 mechanism (e.g., influenza, Ebola, RSV, SARS, Dengue, and West Nile viruses). Our
12 resistance capacitor design strategy may also be generally applicable for treating other
13 rapidly evolving diseases, especially when combined with recent advances in
14 anticipating likely structural sources of drug resistance (37). Finally, the development of
15 PIE12-trimer as a strong clinical candidate will allow D-peptide therapeutics to be
16 evaluated *in vivo* to determine if their theoretical advantages warrant a prominent role
17 as a new class of therapeutic agents.

1 **Experimental Procedures**

2 **Peptide synthesis**

3 All peptides were synthesized as described (57). Dimers and trimers were made
4 essentially as described using bis-dPEG₅ NHS Ester (Quanta BioDesign, catalog no.
5 10224) except for PIE12-trimer, which was synthesized using the following higher yield
6 protocol. PIE12-GK (2 mM) was reacted with bis-dPEG₅ NHS ester crosslinker (1 M
7 stock in dimethylacetamide) at a 1:20 (peptide:PEG) molar ratio in 100 mM HEPES (pH
8 7.8-8) for 90 seconds at RT. The reaction was stopped by addition of acetic acid to 5%
9 and 3 M GuHCl and purified by RP-HPLC (C18, Vydac). This product (~3-5 mM) was
10 reacted at a 2:1 molar excess with PIE12-GKK in dimethylacetamide buffered by
11 triethylamine (pH 7.5) for 75 minutes and purified by RP-HPLC (C18, Vydac).

12

13 **Phage Display vector design**

14 Use of a commercially available phage library cloning system (NEB) allowed us to
15 relocate cloning sites away from the flanking regions (38). We redesigned the regions
16 immediately outside the flanking residues in our cloning vector in order to structurally
17 isolate them and minimize any bias caused by flanking sequence randomization. Our
18 library peptides are displayed as fusions to the phage p3 protein, which contains an N-
19 terminal leader sequence that is cleaved by *E. coli* secretion signal peptidases. In the
20 original vector, the N-terminal flanking residues of the library peptides are immediately
21 adjacent to the secretion signal. Due to proximity to the secretion signal cleavage site, it
22 is likely that randomization of these residues would differentially affect library-p3 protein
23 secretion and peptide presentation on the phage surface. This bias would confound the

1 selection of N-terminal flanking sequences based solely on their affinity for the N-trimer.
2 To avoid this bias, we introduced a five amino acid spacer to structurally isolate the
3 cleavage site from the randomized N-terminal flanking residues. We choose the N-
4 terminal residues (KIEEG) from maltose binding protein (MBP) as the spacer sequence,
5 since MBP is very efficiently cleaved during secretion from *E. coli*.

6 We have observed that mutations in the C-terminal sequence that links the peptide
7 to the phage p3 protein can also create undesirable selection bias (presumably by
8 allowing the C-terminus of the D-peptides to form a continuous helix with the N-terminus
9 of p3, thus enhancing peptide presentation to the target) (57). Therefore, a flexible
10 GGGs spacer was inserted after the C-terminal flanking residues to structurally isolate
11 them from the N-terminus of p3.

12 To validate this new phage display vector, we used it to clone an earlier generation
13 PIE (PIE2) along with a mutant (PIE2-AAA), which had been previously observed to
14 enhance phage affinity for the pocket target via mutation of the linker between the
15 library peptide and p3, although this mutation did not enhance inhibitor potency when
16 incorporated into a D-peptide (57). We assayed the target binding affinity of the
17 resultant phage (Φ) and compared it to phage produced with the previous phage vector.
18 In the previous phage vector, the PIE2-AAA- Φ “cheated” in order to bind the target with
19 ~70-fold more affinity compared to PIE2- Φ , but this difference was abolished in the
20 modified vector (data not shown). Furthermore, sequencing revealed that N-terminal
21 flanking residues from the amplified phage library prior to selection were random,
22 indicating a lack of bias due to signal peptidase cleavage efficiency.

23

1

2 Phage Display

3 8-mer flanking library phage display was performed essentially as described (57).

4 Four rounds of mirror image solution-phase phage display were performed by
5 incubating (for 2 hours at RT) 10^{10} phage (amplified from the previous round) with 10
6 nM biotinylated D-IZN17 in the presence of escalating soluble competitor (L-2K-PIE2)
7 (10, 30, 90, and 360 μM for rounds 1-4, respectively) (57). Phage-bound D-IZN17 was
8 rapidly captured from solution using Dynal T1 streptavidin-coated magnetic beads
9 (Invitrogen) and briefly washed 3X with 500 μL of 0.1% Tween-20 in TBS (wash buffer
10 contained 100 μM D-biotin for the 1st wash). Phage were eluted in 50 μL of glycine (pH
11 2.2) elution buffer (10 min at RT) and neutralized with 7.5 μL of 1M Tris pH 9.1. The
12 amplified phage library was sequenced prior to the first round of selection to confirm
13 randomization, and pre-amplified eluted phage were sequenced following each round.
14 All phage binding experiments were performed using the same protocol as that
15 described above using 270 μM L-PIE2 soluble competitor. 7-mer phage display was
16 performed using a similar protocol.

17

18 Crystal growth and data collection

19 The original form of PIE12 (Table 1) contains a C-terminal -GK extension and did
20 not yield highly diffracting crystals in complex with IQN17. Variants of PIE12 instead
21 containing an N-terminal K- or KG- extension (K-PIE12: KHPCDYPEWQWLCEL and
22 KG-PIE12: KGHPCDYPEWQWLCEL) crystallized in complex with IQN17 under a
23 variety of conditions. In each case, the reservoir (850 μL) comprised a solution from a

1 commercially available crystallization screen and the crystallization drop was prepared
2 by mixing 0.3 or 0.5 μ L of the IQN17-PIE12 or IQN17-PIE71 protein solution (1:1.1
3 molar ratio, 10 mg/mL total in water) with 0.3 μ L of the reservoir solution. Crystals
4 typically grew in 1 to 10 days. All crystals were grown by sitting drop vapor diffusion.
5 IQN17-PIE12 Form I crystals (KG-PIE12) were grown at 21 °C in Hampton Scientific
6 condition Screen II #48 (10% PEG 20,000, 0.1 M bicine pH 9.0, 2% dioxane). IQN17-
7 PIE12 Form II crystals (KG-PIE12) were grown at 21 °C in Emerald Biosystems
8 condition Cryo-II #37 (50% ethylene glycol, 0.1 M imidazole pH 8.0). IQN17-PIE12 Form
9 III crystals (K-PIE12) were grown at 4 °C in Emerald Biosystems condition Cryo-II #25
10 (40% MPD, 0.1 M CAPS pH 10.5). IQN17-PIE71 crystals were grown at 21 °C in
11 QIAGEN PACT crystallization condition #G4 (20% Peg 3350, 0.2 M Potassium
12 Thiocyanate, 0.1 M Bis Tris Propane pH 7.5).

13 Crystals were mounted in a nylon loop and either cryo-cooled directly by plunging
14 into liquid nitrogen or cryo-cooled following brief (20 s) immersion in 20 μ L crystallization
15 buffer with 30% (IQN17-PIE12) or 15% (IQN17-PIE71) added glycerol. Crystals were
16 maintained at 100 K during data collection. Data were collected either in-lab using a
17 rotating copper anode X-ray generator or at a synchrotron beam line. Data were
18 processed using DENZO and SCALEPACK (40). All structures were determined by
19 molecular replacement using PHASER (33) with IQN17-PIE7 as the search model. The
20 models were rebuilt using O (25) and refined against a maximum likelihood target
21 function using REFMAC (36). Structures were checked using MolProbity (6). Data and
22 refinement statistics are indicated in Table 2.

23

1 **Explanation of Lys placement**

2 We were concerned that direct C-terminal addition of Lys would not be well
3 tolerated because the D-peptide C-terminal region forms an α -helix critically involved in
4 the pocket-binding interface, with the C-terminus itself being amidated for helix stability.
5 Therefore, we inserted a Gly between the original C-terminus of PIE7 and the C-
6 terminal Lys, both to cap the helix and separate the Lys from the binding interface.
7 Unexpectedly, the PIE7-GK monomer is slightly more potent than PIE7 (Table 1). A
8 version of PIE7, containing an N- and C-terminal Lys (K-PIE7-GK), has the same
9 potency as PIE7-GK (data not shown), indicating a beneficial effect imposed by the C-
10 terminal Gly-Lys as opposed to a deleterious effect created by a single Lys at the N-
11 terminus. This benefit is likely the reason that the C₅C linkage results in slightly superior
12 potency compared to the N₅C linkage (Table 1).

13

14 **Viral infectivity assays**

15 Pseudovirion infectivity assays were performed as previously described (57). Purified
16 lyophilized inhibitors were dissolved in water (monomers) or 50 mM HEPES pH 7.5
17 (dimers and trimers) to make high concentration stocks. For HEPES-containing
18 samples, all media were adjusted to match the HEPES content of the highest
19 concentration sample (typically ~ 1 mM). HEPES at higher concentrations (e.g., 3 mM)
20 enhanced infectivity up to ~15% but had minimal effect at ≤ 0.5 mM. The Monogram
21 PhenoSense Entry and PBMC assays were performed as previously described (43, 52).

22

23 **Circular Dichroism Studies**

1 Samples were prepared with 2 μ M IZN17, 1.1x molar ratio of inhibitor to target
2 binding sites, PBS (50 mM sodium phosphate, 150 mM NaCl, pH 7.4), and 2M GuHCl in
3 a total volume of 2.5 mL. Thermal melts were performed by melting the sample in a
4 square 1 cm cuvette from 25°C to 90°C (or 93°C for PIE12-trimer) in 2°C increments,
5 with 2 minute equilibration. To show reversibility, reverse melts were performed on each
6 sample from 90°C to 30°C in 10°C increments, with 5 minute equilibration. Data were
7 averaged from a 30 s collection on an Aviv Model 410 Circular Dichroism
8 Spectrapolarimeter.

9 For each sample the CD data followed a smooth sigmoid transition as the sample
10 was heated or cooled. The data were smoothed in Kaleidagraph (Synergy Software)
11 using 2 points from both sides. The derivative value of the smoothed data was used to
12 determine the point with the steepest rate of change on the melt curve, which is the
13 melting temperature (T_m).

14

15 **Passaging Studies**

16 Laboratory-adapted HIV-1 strain NL4-3 was generated by transient transfection of
17 proviral DNA (pNL4-3) into 293T cells using Lipofectamine (Invitrogen). Cell-free
18 supernatants containing virus were collected 48 hours post-transfection and used to
19 infect 5×10^5 CEM-1 cells in RPMI 1640 media (0.5 ml). Virus was serially propagated
20 once a week by a 1:5 dilution of cell-free viral supernatants into fresh CEM-1 cells
21 (5×10^5 cells, 0.5 ml) in the absence or presence of inhibitor (PIE7-dimer, PIE12-dimer or
22 PIE12-trimer). Viral titers were monitored biweekly by p24 antigen ELISA (PerkinElmer).
23 Inhibitor concentration started at \sim IC₅₀ concentrations (20 nM for PIE7-dimer; 1 nM for

1 PIE12-dimer and PIE12-trimer) and raised 1.5 to 2-fold when p24 antigen levels in
2 inhibitor-containing cultures approached that of inhibitor-free cultures (usually 2-3 wk for
3 PIE7-dimer). PIE12-dimer and PIE12-trimer required a slower escalation strategy with
4 prolonged incubation at fixed inhibitor concentration for 5-15 weeks before escalation.

5 To identify PIE7-dimer-escape mutations, viral RNA was isolated from cell-free
6 supernatants of at least two cultures independently propagated either in the presence
7 (resistant virus) or absence (control virus) of inhibitor (Qiagen RNA Purification Kit).
8 Env cDNA was generated by reverse transcription (Eppendorf cMaster RTplus system
9 and cMaster RT Kit), amplified by PCR, and sequenced in five stretches (Thomas
10 Jefferson University Nucleic Acid Facility). To confirm selected mutations in the gp41
11 N-peptide region, the cDNA segment encoding the gp41 ectodomain was reamplified by
12 PCR and subcloned into the pAED4 vector, and the plasmid DNA from three or more
13 individual clones was sequenced. The substitutions E560K and V570I were observed in
14 all sequences from PIE7-dimer resistant virus, but not observed in any sequence from
15 control virus. An expression plasmid for HXB2 Env (pEBB_HXB2 Env) incorporating
16 these substitutions was generated using site-directed mutagenesis (QuickChange,
17 Stratagene) and utilized in the pseudoviral infectivity assay described above.

18

19 **Accession Numbers**

20 Protein Data Bank entry codes for the PIE12:IQN17 complex are 3L35, 3L36,
21 and 3L37 for crystal forms I, II, and III, respectively, and 3MGN for the PIE71:IQN17
22 complex.

1 **Acknowledgements**

2 We thank Bob Schackmann and Scott Endicott (U. of Utah Peptide Synthesis
3 Core Facility) for peptide synthesis, Yu Shi for early 7-mer phage display, and Dong
4 Han and Pham Phung (Monogram) for technical assistance with the PhenoSense Entry
5 assay. PBMC assays were performed by Southern Research Institute (Roger Ptak, PI)
6 funded by contract HHSN272200700041C (National Institute of Allergy and Infectious
7 Diseases, National Institutes of Health, Department of Health and Human Services).

8 This work was supported by grants from the NIH to M.S.K (AI076168), M.J.R.
9 (GM066682), and C.P.H. (GM082545), as well as a U. of Utah Technology
10 Commercialization Grant to M.S.K. Portions of this research were carried out at the
11 Stanford Synchrotron Radiation Lightsource, a national user facility operated by
12 Stanford University on behalf of the U.S. Department of Energy, Office of Basic Energy
13 Sciences. The SSRL Structural Molecular Biology Program is supported by the
14 Department of Energy, Office of Biological and Environmental Research, and by the
15 NIH, National Center for Research Resources, Biomedical Technology Program, and
16 the NIGMS.

17 BDW, DME, and MSK are co-founders of Kayak Biosciences. This startup
18 company is focused on advancing D-peptide inhibitors to the clinic.

19
20
21

1 **Table 1. D-peptide inhibition data**

Sample	Sequence	IC ₅₀ (nM) [†] (HXB2)	IC ₅₀ (nM) [†] (JRFL)
PIE7	KGA[PIE7]AA	620 [§]	2400 [§]
PIE7-GK	GA[PIE7]AAGK	390	16000
PIE7-GKK	GA[PIE7]AAGKK	380	19000
PIE12	HP[PIE7]ELGK	37	580
PIE13 [‡]	HP[PIE7]KL	41	1500
PIE14	HP[PIE7]RLGK	33	1100
PIE15	HA[PIE7]ELGK	67	1400
N ₉ N(PIE7) ₂	(KGA[PIE7]AA) ₂	1.9 [§]	2300 [§]
N ₅ C(PIE7) ₂	GA[PIE7]AAGK-KGA[PIE7]AA	0.6	300
C ₅ C(PIE7) ₂	(GA[PIE7]AAGK) ₂	0.5	200
C ₅ C(PIE12) ₂	(HP[PIE7]ELGK) ₂	0.4	14
N ₉ N(PIE7) ₃	(KGA[PIE7]AA) ₃	0.3 [§]	220 [§]
C ₅ C(PIE7) ₃	(GA[PIE7]AAGK) ₃	0.1	6.7
C ₅ C(PIE12) ₃	(HP[PIE7]ELGK) ₃	0.5	2.8
C37	-	1.4 [§]	13 [§]
Fuzeon	-	3.7 [§]	5.0 [§]

2 [†]IC₅₀ s.e.m. is <25% for duplicate assays for all values3 [§]Values from (57)4 [‡]PIE13 does not include a C-terminal -GK extension because its C-terminal flanking sequence contains a Lys

5 residue

6 *Central peptide of each trimer has two tandem Lys residues (not shown)

7 [PIE7] = CDYPEWQWLC = PIE7 core motif

1 **Table 2: PIE12 and PIE71 crystallographic data and refinement statistics**

Data	PIE12 Form I	PIE12 Form II	PIE12 Form III	PIE71
Crystal	PIE12 Form I	PIE12 Form II	PIE12 Form III	PIE71
Space Group	P2 ₁	R3	P321	P2 ₁
Resolution (Å)	30.0 – 1.55	30.0 – 1.45	30.0 – 1.45	30.0 – 1.40
Resolution (Å) (high-resolution shell)	(1.61 – 1.55)	(1.50 – 1.45)	(1.50 – 1.45)	(1.45 – 1.40)
# Reflections measured	113,335	98,687	186,351	468,599
# Unique reflections	25,088	10,475	14,802	82,774
Redundancy	4.5	9.4	12.6	5.7
Completeness (%)	86.5 (66.8)	97.1 (80.1)	99.7 (96.6)	98.2 (97.6)
<I/σI>	18 (2.4)	19 (3.1)	17 (2.7)	15 (2.0)
Mosaicity (°)	0.44	0.37	0.45	0.29
Rsym ^a	0.051 (0.250)	0.058 (0.102)	0.107 (0.235)	0.052 (0.316)
Refinement				
Resolution (Å)	30.0 – 1.55	30.0 – 1.45	30.0 – 1.45	30.0 – 1.40
Resolution (Å) – (high-resolution shell)	(1.59 – 1.55)	(1.49 – 1.45)	(1.49 – 1.45)	(1.44 – 1.40)
# Reflections used for refinement	23,765	9,448	13,629	80,532
# Reflections in Rfree set	1,273	1,026	1,136	1,654
Rcryst ^b	0.232 (0.465)	0.234 (0.301)	0.243 (0.299)	0.261 (0.306)
Rfree ^c	0.288 (0.624)	0.264 (0.392)	0.278 (0.350)	0.288 (0.335)
RMSD: bonds (Å) / angles (°)	0.012 / 1.440	0.013 / 1.693	0.010 / 1.530	0.009 / 1.094
 (Å ²): all atoms / # atoms	23.7 / 1172	31.9 / 384	29.2 / 384	Mol 1 – 24.3/1555 Mol 2 – 36.0/1491
 (Å ²): PIE12 only / # atoms	21.3 / 420	30.8 / 144	25.9 / 144	Mol 1 – 18.3/368 Mol 2 – 39.9/322
 (Å ²): water molecules / #water	32.0 / 197	38.0 / 36	40.6 / 49	39.9 / 389
φ/ψ most favored (%)	100	98.1	100	99.0

2 Values in parenthesis refer to data in the high resolution shell.

3 ^a Rsym = $\sum |I - \langle I \rangle| / \sum I$ where I is the intensity of an individual measurement and $\langle I \rangle$ is the corresponding mean value.4 ^b Rcryst = $\sum ||F_o| - |F_c|| / \sum |F_o|$, where $|F_o|$ is the observed and $|F_c|$ the calculated structure factor amplitude.5 ^c Rfree is the same as Rcryst calculated with a randomly selected test set of reflections that were never used in
6 refinement calculations.

7

1 **Table 3. PhenoSense entry assay data**

HIV-1 Isolate	Subtype	IC ₅₀ (nM) PIE7 Trimer	IC ₅₀ (nM) PIE12 Trimer	IC ₅₀ (nM) PIE12 Monomer	IC ₅₀ (nM) Fuzeon
A*	A	5.5	4.1	2,300	18
92RW008	A	2.0	1.0	1,400	7.2
92UG031	A	18	4.2	2,600	20
94KE105	AC	16	0.7	1,900	13
CMU02	AE	32	12	1,500	16
B*	B	140	13	3,300	30
1168	A	54	31	4,700	140.0
BaL	B	2.0	2.5	1,700	10
ENFr1*	B	2.0	0.8	790	760
ENFr2*	B	0.7	1.0	300	5,400
HXB2	B	0.1	0.3	50	2.6
JRCSF	B	13	3.4	1,100	14
JRFL	B	21	5.7	1,900	7.9
NL4.3	B	0.3	0.4	150	62
SF162	B	3.4	4.5	940	34
98CN009	BC	0.4	0.4	320	7.9
93BR029	BF	1.5	0.9	750	12
C*	C	220.0	26	5,100	71
97ZA012	C	2.0	0.7	1,500	10
98IN022	C	1.1	1.1	820	6.9
21068	C	6.6	5.0	1,800	47
D*	D	3.1	3.2	820	17
92UG005	D	3.9	2.5	2,000	10
aMLV	---	>10,000	>10,000	>500,000	>15,000

2 * Polyclonal viral envelopes amplified from patient plasma

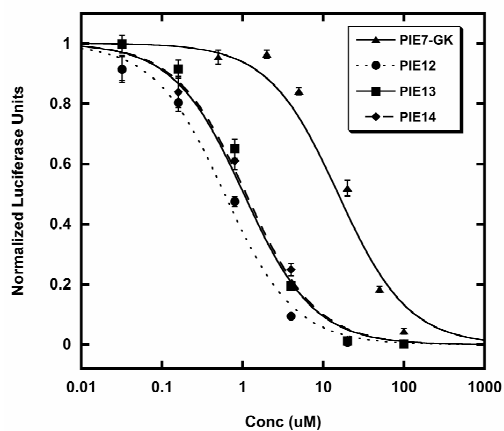
3

4

1 **Table 4. PBMC assay data**

HIV-1 Isolate	Subtype	IC ₅₀ (nM) PIE7 Trimer	IC ₅₀ (nM) PIE12 Trimer	IC ₅₀ (nM) PIE12 Monomer	IC ₅₀ (nM) Fuzeon
92UG029	A	1.6	0.7	290	190
92UG037	A	0.1	0.2	36	41
93TH073	AE	0.6	0.8	270	200
CMU02	AE	0.2	0.4	300	44
CMU06	AE	0.3	0.4	210	5.7
IIIB	B	0.3	0.8	140	28
BaL	B	0.2	0.3	72	20
JRCSF	B	0.1	0.1	120	7.0
JRFL	B	0.5	0.3	110	1.7
93BR019	BF	1.7	4.7	170	>1,000
92BR025	C	15	5.2	>1,000	310
93IN101	C	0.4	0.4	160	22
92UG001	D	0.8	4.5	230	180
92UG046	D	0.1	1.2	170	130
93BR020	F	0.2	0.4	190	59
93BR029	F	0.2	0.8	86	19
G3	G	0.3	1.2	310	23
RU570	G	0.3	0.4	480	37
BCF01	Group O	>1,000	>1,000	>1,000	330
BCF02	Group O	>1,000	440	>1,000	0.4

2
3
4
5

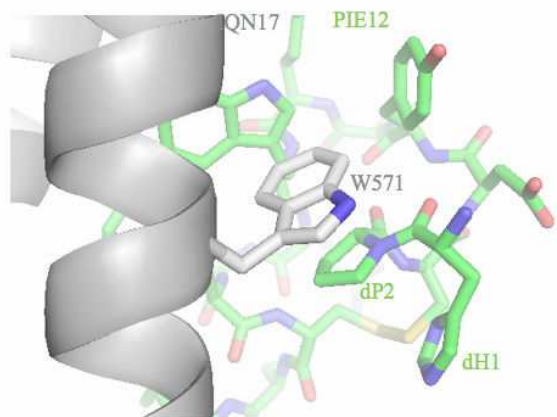
1
2

3

4 **Figure 1.** Optimization of flanking residues enhances PIE potency. Each point
5 represents the average of quadruplicate measurements from a representative
6 pseudovirion entry inhibition assay (JRFL strain) normalized to uninhibited control. Error
7 bars represent the SEM. (A) PIE12 is ~2-fold more potent than PIE13 or PIE14 and is
8 ~25-fold more potent than PIE7-GK.

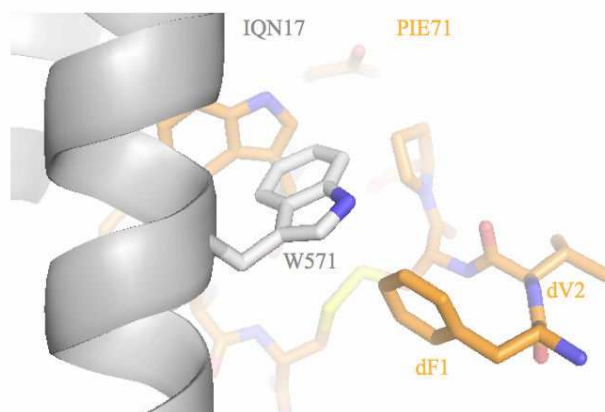
9

1



2

3 **Figure 2.** Crystal structure of PIE12 binding to IQN17. Trp571 of the gp41 pocket (gray)
4 and the N-terminal flank residues (dH1 and dP2) of PIE12 (green) appear to stabilize
5 binding via ring-stacking interactions. Disulfide bond (yellow) is shown in the
6 background.

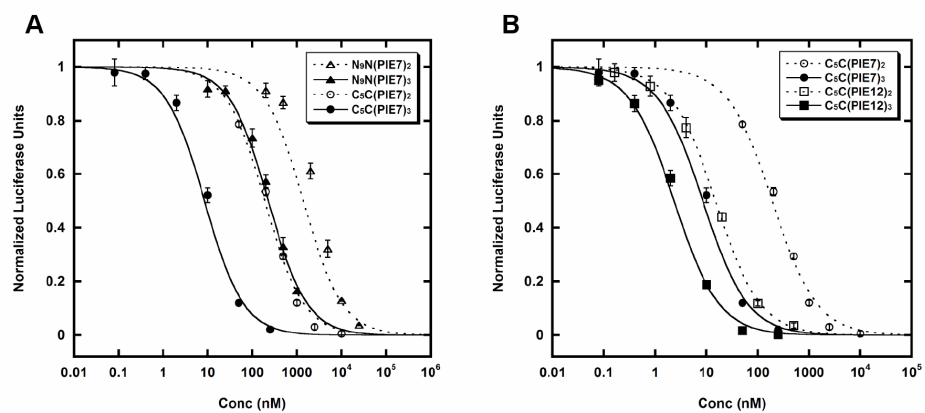


1

2 **Figure 3.** Crystal structure of PIE71 binding to IQN17. The N-terminal flank residues
3 (dF1 and dV2) of PIE71 (orange) are directed away from the pocket compared to PIE12
4 (see Fig. 2). Disulfide bond (yellow) is shown in the background.

5

1

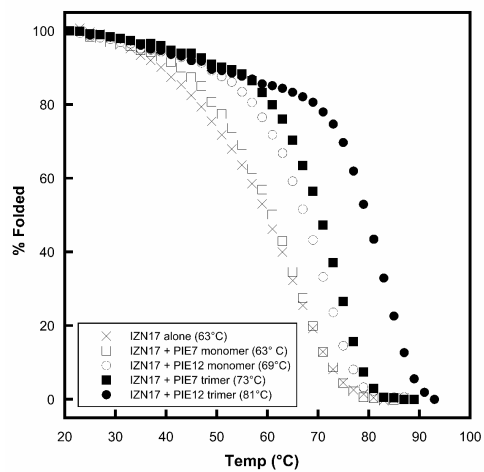


2

3 **Figure 4.** Optimization of linkage geometry. Each point represents the average of
 4 quadruplicate measurements from a representative pseudovirion entry inhibition assay
 5 (JRFL strain) normalized to uninhibited control. Error bars represent the SEM. (A)
 6 Comparison of N₉N to C₅C linkages. (B) PIE7 vs. PIE12 dimers and trimers (all C₅C
 7 linkages).

8

1



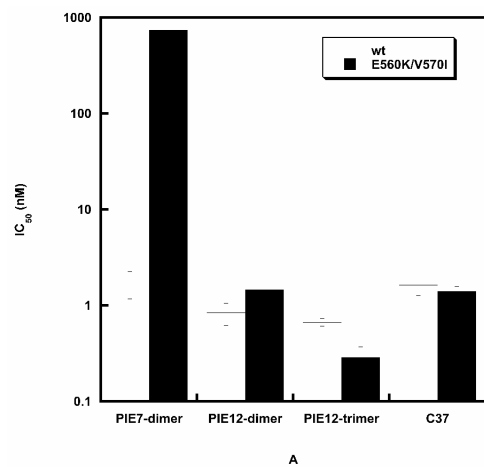
2

3 **Figure 5.** Stability of D-peptide complexes. Normalized melting curves of IZN17 alone4 and with D-peptide inhibitors monitored by CD in PBS + 2 M GuHCl. T_m values are

5 indicated in the legend.

6

1



2

3 **Figure 6.** Effect of PIE7-dimer resistance mutations on PIE7-dimer, PIE12-dimer, and
4 PIE12-trimer potency. IC₅₀ values against wt and PIE7-dimer resistant (E560K/V570I)
5 HXB2 pseudovirion entry are shown. The C-peptide inhibitor C37 is included as a
6 control. Data represent the mean from at least two independent experiments. Error bars
7 represent the SEM.

1 **References**

- 2 1. **Buonaguro, L., M. L. Tornesello, and F. M. Buonaguro.** 2007. Human immunodeficiency virus
3 type 1 subtype distribution in the worldwide epidemic: pathogenetic and therapeutic
4 implications. *J Virol* **81**:10209-19.
- 5 2. **Chan, D. C., C. T. Chutkowski, and P. S. Kim.** 1998. Evidence that a prominent cavity in the
6 coiled coil of HIV type 1 gp41 is an attractive drug target. *Proc Natl Acad Sci U S A* **95**:15613-7.
- 7 3. **Chan, D. C., D. Fass, J. M. Berger, and P. S. Kim.** 1997. Core structure of gp41 from the HIV
8 envelope glycoprotein. *Cell* **89**:263-73.
- 9 4. **Chinnadurai, R., D. Rajan, J. Munch, and F. Kirchhoff.** 2007. Human immunodeficiency virus
10 type 1 variants resistant to first- and second-generation fusion inhibitors and cytopathic in ex vivo
11 human lymphoid tissue. *J Virol* **81**:6563-72.
- 12 5. **Cooper, D. A., R. T. Steigbigel, J. M. Gatell, J. K. Rockstroh, C. Katlama, P. Yeni, A. Lazzarin, B.**
13 **Clotet, P. N. Kumar, J. E. Eron, M. Schechter, M. Markowitz, M. R. Loutfy, J. L. Lennox, J. Zhao,**
14 **J. Chen, D. M. Ryan, R. R. Rhodes, J. A. Killar, L. R. Gilde, K. M. Strohmaier, A. R. Meibohm, M.**
15 **D. Miller, D. J. Hazuda, M. L. Nessler, M. J. DiNubile, R. D. Isaacs, H. Teppler, and B. Y. Nguyen.**
16 2008. Subgroup and resistance analyses of raltegravir for resistant HIV-1 infection. *N Engl J Med*
17 **359**:355-65.
- 18 6. **Davis, I. W., A. Leaver-Fay, V. B. Chen, J. N. Block, G. J. Kapral, X. Wang, L. W. Murray, W. B.**
19 **Arendall, 3rd, J. Snoeyink, J. S. Richardson, and D. C. Richardson.** 2007. MolProbity: all-atom
20 contacts and structure validation for proteins and nucleic acids. *Nucleic Acids Res* **35**:W375-83.
- 21 7. **Debnath, A. K., L. Radigan, and S. Jiang.** 1999. Structure-based identification of small molecule
22 antiviral compounds targeted to the gp41 core structure of the human immunodeficiency virus
23 type 1. *J Med Chem* **42**:3203-9.
- 24 8. **Derdeyn, C. A., J. M. Decker, J. N. Sfakianos, Z. Zhang, W. A. O'Brien, L. Ratner, G. M. Shaw,**
25 **and E. Hunter.** 2001. Sensitivity of human immunodeficiency virus type 1 to fusion inhibitors
26 targeted to the gp41 first heptad repeat involves distinct regions of gp41 and is consistently
27 modulated by gp120 interactions with the coreceptor. *J Virol* **75**:8605-14.
- 28 9. **Dwyer, J. J., K. L. Wilson, D. K. Davison, S. A. Freel, J. E. Sedorff, S. A. Wring, N. A. Tvermoes,**
29 **T. J. Matthews, M. L. Greenberg, and M. K. Delmedico.** 2007. Design of helical, oligomeric HIV-1
30 fusion inhibitor peptides with potent activity against enfuvirtide-resistant virus. *Proc Natl Acad Sci U S A* **104**:12772-7.
- 31 10. **Eckert, D. M., and P. S. Kim.** 2001. Design of potent inhibitors of HIV-1 entry from the gp41 N-
32 peptide region. *Proc Natl Acad Sci U S A* **98**:11187-92.
- 33 11. **Eckert, D. M., and P. S. Kim.** 2001. Mechanisms of viral membrane fusion and its inhibition.
34 *Annu Rev Biochem* **70**:777-810.
- 35 12. **Eckert, D. M., V. N. Malashkevich, L. H. Hong, P. A. Carr, and P. S. Kim.** 1999. Inhibiting HIV-1
36 entry: discovery of D-peptide inhibitors that target the gp41 coiled-coil pocket. *Cell* **99**:103-15.
- 37 13. **Eggink, D., C. E. Baldwin, Y. Deng, J. P. Langedijk, M. Lu, R. W. Sanders, and B. Berkhout.** 2008.
38 Selection of T1249-resistant human immunodeficiency virus type 1 variants. *J Virol* **82**:6678-88.
- 39 14. **Ernst, J. T., O. Kutzki, A. K. Debnath, S. Jiang, H. Lu, and A. D. Hamilton.** 2002. Design of a
40 protein surface antagonist based on alpha-helix mimicry: inhibition of gp41 assembly and viral
41 fusion. *Angew Chem Int Ed Engl* **41**:278-81.
- 42 15. **Ferrer, M., T. M. Kapoor, T. Strassmaier, W. Weissenhorn, J. J. Skehel, D. Orian, S. L.**
43 **Schreiber, D. C. Wiley, and S. C. Harrison.** 1999. Selection of gp41-mediated HIV-1 cell entry
44 inhibitors from biased combinatorial libraries of non-natural binding elements. *Nat Struct Biol*
45 **6**:953-60.
- 46

- 1 16. **Freed, E. O., and M. A. Martin.** 1995. The role of human immunodeficiency virus type 1
2 envelope glycoproteins in virus infection. *J Biol Chem* **270**:23883-6.
- 3 17. **Frey, G., S. Rits-Volloch, X. Q. Zhang, R. T. Schooley, B. Chen, and S. C. Harrison.** 2006. Small
4 molecules that bind the inner core of gp41 and inhibit HIV envelope-mediated fusion. *Proc Natl*
5 *Acad Sci U S A* **103**:13938-43.
- 6 18. **Furuta, R. A., C. T. Wild, Y. Weng, and C. D. Weiss.** 1998. Capture of an early fusion-active
7 conformation of HIV-1 gp41. *Nat Struct Biol* **5**:276-9.
- 8 19. **Gao, F., E. Bailes, D. L. Robertson, Y. Chen, C. M. Rodenburg, S. F. Michael, L. B. Cummins, L. O.**
9 **Arthur, M. Peeters, G. M. Shaw, P. M. Sharp, and B. H. Hahn.** 1999. Origin of HIV-1 in the
10 chimpanzee *Pan troglodytes troglodytes*. *Nature* **397**:436-41.
- 11 20. **Gaschen, B., J. Taylor, K. Yusim, B. Foley, F. Gao, D. Lang, V. Novitsky, B. Haynes, B. H. Hahn, T.**
12 **Bhattacharya, and B. Korber.** 2002. Diversity considerations in HIV-1 vaccine selection. *Science*
13 **296**:2354-60.
- 14 21. **Golding, H., M. Zaitseva, E. de Rosny, L. R. King, J. Manischewitz, I. Sidorov, M. K. Gorny, S.**
15 **Zolla-Pazner, D. S. Dimitrov, and C. D. Weiss.** 2002. Dissection of human immunodeficiency
16 virus type 1 entry with neutralizing antibodies to gp41 fusion intermediates. *J Virol* **76**:6780-90.
- 17 22. **Jiang, S., K. Lin, N. Strick, and A. R. Neurath.** 1993. HIV-1 inhibition by a peptide. *Nature*
18 **365**:113.
- 19 23. **Jiang, S., H. Lu, S. Liu, Q. Zhao, Y. He, and A. K. Debnath.** 2004. N-substituted pyrrole derivatives
20 as novel human immunodeficiency virus type 1 entry inhibitors that interfere with the gp41 six-
21 helix bundle formation and block virus fusion. *Antimicrob Agents Chemother* **48**:4349-59.
- 22 24. **Jin, B. S., J. R. Ryu, K. Ahn, and Y. G. Yu.** 2000. Design of a peptide inhibitor that blocks the cell
23 fusion mediated by glycoprotein 41 of human immunodeficiency virus type 1. *AIDS Res Hum*
24 *Retroviruses* **16**:1797-804.
- 25 25. **Jones, T. A., J. Y. Zou, S. W. Cowan, and M. Kjeldgaard.** 1991. Improved methods for building
26 protein models in electron density maps and the location of errors in these models. *Acta*
27 *Crystallogr A* **47 (Pt 2)**:110-9.
- 28 26. **Judice, J. K., J. Y. Tom, W. Huang, T. Wrin, J. Vennari, C. J. Petropoulos, and R. S. McDowell.**
29 1997. Inhibition of HIV type 1 infectivity by constrained alpha-helical peptides: implications for
30 the viral fusion mechanism. *Proc Natl Acad Sci U S A* **94**:13426-30.
- 31 27. **Kahle, K. M., H. K. Steger, and M. J. Root.** 2009. Asymmetric Deactivation of HIV-1 gp41
32 following Fusion Inhibitor Binding. *PLoS Pathog* **5**:e1000674.
- 33 28. **Kobayashi, M., K. Nakahara, T. Seki, S. Miki, S. Kawauchi, A. Suyama, C. Wakasa-Morimoto, M.**
34 **Kodama, T. Endoh, E. Oosugi, Y. Matsushita, H. Murai, T. Fujishita, T. Yoshinaga, E. Garvey, S.**
35 **Foster, M. Underwood, B. Johns, A. Sato, and T. Fujiwara.** 2008. Selection of diverse and
36 clinically relevant integrase inhibitor-resistant human immunodeficiency virus type 1 mutants.
37 *Antiviral Res* **80**:213-22.
- 38 29. **Lalezari, J. P., N. C. Bellos, K. Sathasivam, G. J. Richmond, C. J. Cohen, R. A. Myers, Jr., D. H.**
39 **Henry, C. Raskino, T. Melby, H. Murchison, Y. Zhang, R. Spence, M. L. Greenberg, R. A. Demasi,**
40 **and G. D. Miralles.** 2005. T-1249 retains potent antiretroviral activity in patients who had
41 experienced virological failure while on an enfuvirtide-containing treatment regimen. *J Infect Dis*
42 **191**:1155-63.
- 43 30. **Lalezari, J. P., K. Henry, M. O'Hearn, J. S. Montaner, P. J. Piliero, B. Trottier, S. Walmsley, C.**
44 **Cohen, D. R. Kuritzkes, J. J. Eron, Jr., J. Chung, R. DeMasi, L. Donatucci, C. Drobnes, J.**
45 **Delehanty, and M. Salgo.** 2003. Enfuvirtide, an HIV-1 fusion inhibitor, for drug-resistant HIV
46 infection in North and South America. *N Engl J Med* **348**:2175-85.
- 47 31. **Lazzarin, A., B. Clotet, D. Cooper, J. Reynes, K. Arasteh, M. Nelson, C. Katlama, H. J. Stellbrink,**
48 **J. F. Delfraissy, J. Lange, L. Huson, R. DeMasi, C. Wat, J. Delehanty, C. Drobnes, and M. Salgo.**

- 1 2003. Efficacy of enfuvirtide in patients infected with drug-resistant HIV-1 in Europe and
2 Australia. *N Engl J Med* **348**:2186-95.
- 3 32. **Marx, P. A.** 2005. Unsolved Questions Over the Origin of HIV and AIDS. *ASM News* **71**:15-20.
- 4 33. **McCoy, A. J., R. W. Grosse-Kunstleve, P. D. Adams, M. D. Winn, L. C. Storoni, and R. J. Read.**
5 2007. Phaser crystallographic software. *J. Appl. Cryst.* **40**:658-674.
- 6 34. **Miller, M. D., R. Geleziunas, E. Bianchi, S. Lennard, R. Hrin, H. Zhang, M. Lu, Z. An, P.**
7 **Ingallinella, M. Finotto, M. Mattu, A. C. Finnefrock, D. Bramhill, J. Cook, D. M. Eckert, R.**
8 **Hampton, M. Patel, S. Jarantow, J. Joyce, G. Ciliberto, R. Cortese, P. Lu, W. Strohl, W. Schleif,**
9 **M. McElhaugh, S. Lane, C. Lloyd, D. Lowe, J. Osbourn, T. Vaughan, E. Emini, G. Barbato, P. S.**
10 **Kim, D. J. Hazuda, J. W. Shiver, and A. Pessi.** 2005. A human monoclonal antibody neutralizes
11 diverse HIV-1 isolates by binding a critical gp41 epitope. *Proc Natl Acad Sci U S A* **102**:14759-64.
- 12 35. **Munoz-Barroso, I., S. Durell, K. Sakaguchi, E. Appella, and R. Blumenthal.** 1998. Dilation of the
13 human immunodeficiency virus-1 envelope glycoprotein fusion pore revealed by the inhibitory
14 action of a synthetic peptide from gp41. *J Cell Biol* **140**:315-23.
- 15 36. **Murshudov, G. N., A. A. Vagin, and E. J. Dodson.** 1997. Refinement of macromolecular
16 structures by the maximum-likelihood method. *Acta Crystallogr D Biol Crystallogr* **53**:240-55.
- 17 37. **Nalam, M. N., A. Ali, M. D. Altman, G. S. Reddy, S. Chellappan, V. Kairys, A. Ozen, H. Cao, M. K.**
18 **Gilson, B. Tidor, T. M. Rana, and C. A. Schiffer.** 2010. Evaluating the substrate-envelope
19 hypothesis: structural analysis of novel HIV-1 protease inhibitors designed to be robust against
20 drug resistance. *J Virol* **84**:5368-78.
- 21 38. **Noren, K. A., and C. J. Noren.** 2001. Construction of high-complexity combinatorial phage
22 display peptide libraries. *Methods* **23**:169-78.
- 23 39. **Osmanov, S., C. Pattou, N. Walker, B. Schwardlander, and J. Esparza.** 2002. Estimated global
24 distribution and regional spread of HIV-1 genetic subtypes in the year 2000. *J Acquir Immune*
25 *Defic Syndr* **29**:184-90.
- 26 40. **Otwinowski, Z., and W. Minor.** 1997. Processing of X-ray diffraction data collected in oscillation
27 mode. *Methods in Enzymology* **276**:307-326.
- 28 41. **Pappenheimer, J. R., C. E. Dahl, M. L. Karnovsky, and J. E. Maggio.** 1994. Intestinal absorption
29 and excretion of octapeptides composed of D amino acids. *Proc Natl Acad Sci U S A* **91**:1942-5.
- 30 42. **Pappenheimer, J. R., M. L. Karnovsky, and J. E. Maggio.** 1997. Absorption and excretion of
31 undegradable peptides: role of lipid solubility and net charge. *J Pharmacol Exp Ther* **280**:292-
32 300.
- 33 43. **Petropoulos, C. J., N. T. Parkin, K. L. Limoli, Y. S. Lie, T. Wrin, W. Huang, H. Tian, D. Smith, G. A.**
34 **Winslow, D. J. Capon, and J. M. Whitcomb.** 2000. A novel phenotypic drug susceptibility assay
35 for human immunodeficiency virus type 1. *Antimicrob Agents Chemother* **44**:920-8.
- 36 44. **Ray, N., J. E. Harrison, L. A. Blackburn, J. N. Martin, S. G. Deeks, and R. W. Doms.** 2007. Clinical
37 resistance to enfuvirtide does not affect susceptibility of human immunodeficiency virus type 1
38 to other classes of entry inhibitors. *J Virol* **81**:3240-50.
- 39 45. **Reeves, J. D., S. A. Gallo, N. Ahmad, J. L. Miamidian, P. E. Harvey, M. Sharron, S. Pohlmann, J.**
40 **N. Sfakianos, C. A. Derdeyn, R. Blumenthal, E. Hunter, and R. W. Doms.** 2002. Sensitivity of
41 HIV-1 to entry inhibitors correlates with envelope/coreceptor affinity, receptor density, and
42 fusion kinetics. *Proc Natl Acad Sci U S A* **99**:16249-54.
- 43 46. **Reeves, J. D., F. H. Lee, J. L. Miamidian, C. B. Jabara, M. M. Juntilla, and R. W. Doms.** 2005.
44 Enfuvirtide resistance mutations: impact on human immunodeficiency virus envelope function,
45 entry inhibitor sensitivity, and virus neutralization. *J Virol* **79**:4991-9.
- 46 47. **Rimsky, L. T., D. C. Shugars, and T. J. Matthews.** 1998. Determinants of human
47 immunodeficiency virus type 1 resistance to gp41-derived inhibitory peptides. *J Virol* **72**:986-93.

- 1 48. **Root, M. J., M. S. Kay, and P. S. Kim.** 2001. Protein design of an HIV-1 entry inhibitor. *Science*
2 **291**:884-8.
- 3 49. **Sadowski, M., J. Pankiewicz, H. Scholtzova, J. A. Ripellino, Y. Li, S. D. Schmidt, P. M. Mathews,**
4 **J. D. Fryer, D. M. Holtzman, E. M. Sigurdsson, and T. Wisniewski.** 2004. A synthetic peptide
5 blocking the apolipoprotein E/beta-amyloid binding mitigates beta-amyloid toxicity and fibril
6 formation in vitro and reduces beta-amyloid plaques in transgenic mice. *Am J Pathol* **165**:937-
7 48.
- 8 50. **Schumacher, T. N., L. M. Mayr, D. L. Minor, Jr., M. A. Milhollen, M. W. Burgess, and P. S. Kim.**
9 1996. Identification of D-peptide ligands through mirror-image phage display. *Science* **271**:1854-
10 7.
- 11 51. **Sia, S. K., P. A. Carr, A. G. Cochran, V. N. Malashkevich, and P. S. Kim.** 2002. Short constrained
12 peptides that inhibit HIV-1 entry. *Proc Natl Acad Sci U S A* **99**:14664-9.
- 13 52. **Southern Research Institute** 2008, posting date. Anti-HIV Evaluation Assays in Fresh Human
14 Cells. [Online.]
- 15 53. **Steger, H. K., and M. J. Root.** 2006. Kinetic dependence to HIV-1 entry inhibition. *J Biol Chem*
16 **281**:25813-21.
- 17 54. **Stephens, O. M., S. Kim, B. D. Welch, M. E. Hodsdon, M. S. Kay, and A. Schepartz.** 2005.
18 Inhibiting HIV fusion with a beta-peptide foldamer. *J Am Chem Soc* **127**:13126-7.
- 19 55. **Tan, K., J. Liu, J. Wang, S. Shen, and M. Lu.** 1997. Atomic structure of a thermostable subdomain
20 of HIV-1 gp41. *Proc Natl Acad Sci U S A* **94**:12303-8.
- 21 56. **Weissenhorn, W., A. Dessen, S. C. Harrison, J. J. Skehel, and D. C. Wiley.** 1997. Atomic structure
22 of the ectodomain from HIV-1 gp41. *Nature* **387**:426-30.
- 23 57. **Welch, B. D., A. P. VanDemark, A. Heroux, C. P. Hill, and M. S. Kay.** 2007. Potent D-peptide
24 inhibitors of HIV-1 entry. *Proc Natl Acad Sci U S A* **104**:16828-33.
- 25 58. **Wild, C., J. W. Dubay, T. Greenwell, T. Baird, Jr., T. G. Oas, C. McDanal, E. Hunter, and T.**
26 **Matthews.** 1994. Propensity for a leucine zipper-like domain of human immunodeficiency virus
27 type 1 gp41 to form oligomers correlates with a role in virus-induced fusion rather than
28 assembly of the glycoprotein complex. *Proc Natl Acad Sci U S A* **91**:12676-80.
- 29 59. **Wild, C., T. Greenwell, and T. Matthews.** 1993. A synthetic peptide from HIV-1 gp41 is a potent
30 inhibitor of virus-mediated cell-cell fusion. *AIDS Res Hum Retroviruses* **9**:1051-3.
- 31 60. **Wild, C., T. Oas, C. McDanal, D. Bolognesi, and T. Matthews.** 1992. A synthetic peptide inhibitor
32 of human immunodeficiency virus replication: correlation between solution structure and viral
33 inhibition. *Proc Natl Acad Sci U S A* **89**:10537-41.
- 34 61. **Wild, C. T., D. C. Shugars, T. K. Greenwell, C. B. McDanal, and T. J. Matthews.** 1994. Peptides
35 corresponding to a predictive alpha-helical domain of human immunodeficiency virus type 1
36 gp41 are potent inhibitors of virus infection. *Proc Natl Acad Sci U S A* **91**:9770-4.
- 37
38